

Exploring models of associative memory via cavity quantum electrodynamics

Sarang Gopalakrishnan^a, Benjamin L. Lev^b and Paul M. Goldbart^{c*}

^a*Department of Physics, University of Illinois at Urbana-Champaign, 1110 West Green Street Urbana, Illinois 61801, USA;* ^b*Departments of Applied Physics and Physics and E. L. Ginzton Laboratory, Stanford University, Stanford, CA 94305, USA;* ^c*School of Physics, Georgia Institute of Technology, 837 State Street, Atlanta, GA 30332, USA*

(Received 2 August 2011; final version received 24 October 2011)

Photons in multimode optical cavities can be used to mediate tailored interactions between atoms confined in the cavities. For atoms possessing multiple internal (i.e., “spin”) states, the spin–spin interactions mediated by the cavity are analogous in structure to the Ruderman–Kittel–Kasuya–Yosida (RKKY) interaction between localized spins in metals. Thus, in particular, it is possible to use atoms in cavities to realize models of frustrated and/or disordered spin systems, including models that can be mapped on to the Hopfield network model and related models of associative memory. We explain how this realization of models of associative memory comes about and discuss ways in which the properties of these models can be probed in a cavity-based setting.

Keywords: disordered systems; magnetism; statistical physics; ultracold atoms; neural networks; spin glasses

1. Introductory remarks

Since the development of laser cooling and trapping, a range of phenomena that are traditionally associated with the physics of condensed matter have been realized and explored in ultracold atomic settings [1]. Such realizations differ from their traditional condensed-matter counterparts in their exquisite controllability and tunability: ultracold atomic systems are, as a rule, isolated from the environment and governed by precisely understood microscopic Hamiltonians, in which many of the parameters (including, e.g., interaction strengths) are determined by quantities such as laser intensities, which are readily altered in the course of an experiment. In addition, the ultracold settings offer probes that in the condensed-matter realm either have no parallel or require extraordinary sophistication [2]. For instance, it is possible to image [3,4] and even manipulate [5] ultracold atomic systems at the single-atom level. Because of these features, experiments with ultracold atoms

*Corresponding author. Email: paul.goldbart@physics.gatech.edu

offer a promising setting in which to investigate open questions in many-body physics.

The ubiquity of magnetism and the multitude of puzzles involving it have made realizing models of magnetism a central objective in ultracold atomic physics. Models of magnetism, such as the Heisenberg model, are believed to describe aspects of the phase diagrams of strongly correlated condensed-matter systems such as transition metal oxides; the models are, however, *simplified* descriptions, excluding potentially important degrees of freedom such as phonons. Experiments with ultracold atoms offer the prospect of realizing the theoretically studied models much more precisely; as many of the models are neither exactly solvable nor (owing to “sign problems”) straightforward to study numerically, it is hoped that such experiments (or “quantum emulations”) will shed light on their properties [1].

Perhaps the central effort to realize magnetic ordering, to date, has focused on the fermionic Hubbard model. In this model, the mechanism causing magnetism is antiferromagnetic exchange (often termed “superexchange”) amongst the localized electrons on neighboring lattice sites; however, the temperature scale associated with superexchange is too low to be readily achievable in current experiments [1]. It is therefore desirable to investigate alternative, less direct schemes for exploring magnetism, e.g., by exploiting the analogy between the phase of a Bose–Einstein condensate and the orientation of a planar spin [6], or that between an Ising spin system and a binary fluid [7]. In recent work [8], we introduced an alternative approach, involving atoms having two or more low-lying energy levels that represent the spin states; inter-spin interactions are mediated via virtual photonic excitations of a multimode optical cavity. The central difference between our approach and previous ones lies in the range and structure of interactions: rather than being nearest-neighbor and always of the same sign, the cavity-mediated interactions are longer-ranged (indeed, they are infinite-ranged in the case of a single-mode cavity) and have *alternating* signs, depending on the positions of the spins within the cavity. Thus, the approach discussed in this work is particularly well-suited for studying (a) disordered and/or frustrated spin systems, and (b) spin systems having long-range interactions.

In Ref. [8], we considered a specific atomic configuration that was shown to realize Cook’s generalization to the planar-spin case [9] of the Hopfield neural-network model [10]. The correspondence between the atom–cavity system and the neural-network models was then used to deduce the phase diagram of the former. In particular, we estimated the maximum ratio of the number of cavity modes to the number of spins for which the ground state of the system is a conventionally ordered state that encodes an associative memory; for smaller (larger) numbers of spins (modes), the ground state is expected to be a spin glass [11]. In the present work we take a more general perspective regarding the microscopic degrees of freedom, and address the low-temperature phases, especially the memory-encoding phase, in greater detail. We discuss the origins of frustration in a simple two-cavity-mode model that is related to the van Hemmen model of spins with frustrated interactions [12,13]. We then consider the experimentally accessible channels through which the properties of Hopfield-type models can be investigated in the cavity-based setting.

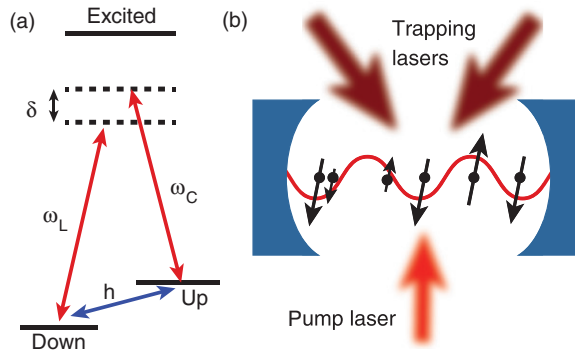


Figure 1. (Color online). (a) A possible atomic level structure for realizing associative memory models with XY spins (see Ref. [8]). The detuning from two-photon resonance δ is assumed to be much smaller than the detuning of both laser and cavity frequencies (ω_L and ω_C respectively) from the atomic transitions. The microwave transition connecting the two spin states can be driven directly; such driving would correspond to the application of a magnetic field h . (b) Experimental setup. Atoms tightly trapped at fixed, random positions by the trapping lasers are pumped by a laser transverse to the cavity axis. The spins are ordered according to one of the patterns (i.e., a cavity mode profile, indicated by the wavy line) stored in the associative memory. Spins at even antinodes interact ferromagnetically with spins at other even antinodes, but antiferromagnetically with spins at odd antinodes. The interactions are strongest (weakest) for atoms located at antinodes (nodes); thus the spins of the atoms at the antinodes are more strongly organized, as depicted.

2. Model and general properties

The general atom–cavity setup involves atoms possessing a ground-state manifold of m low-lying “spin” states (separated from one another by microwave transitions) as well as some number of excited states (separated from the ground-state manifold by much larger, optical transitions). A concrete example, involving a three-level (so-called) Λ atom, is shown in Figure 1a and analyzed in Ref. [8]. The optical transitions are approximately resonant either with pump lasers or with cavity modes; the principle behind the dressing of the atoms with laser and cavity fields is that there should exist nearly resonant processes whereby a photon is scattered from the laser to a cavity mode approximately degenerate with the laser, and the atom simultaneously changes its spin state (i.e., two-photon resonances). In other words, the laser–cavity frequency difference should be close to the spin-state spacings but slightly detuned (by an amount we call δ) below them. Under these conditions, if one ignores dissipative processes, the physical basis for spin–spin interactions can be understood as follows: an atom i can scatter a photon between the laser mode and a cavity mode; in the process, it changes its spin state. The cavity photon, being virtual, must be reabsorbed into the laser on a time-scale $\sim 1/\delta$; this process involves changing the spin state of some atom j , which is in general distinct from atom i . Thus, the process generates an effective spin–spin interaction (generally anisotropic in spin-space) of the form $\delta^{-1} M(\mathbf{x}_i, \mathbf{x}_j) \sum_{\mu} A^{\mu} S_i^{\mu} S_j^{\mu}$ between pairs of atoms. Here, \mathbf{x}_i is the position of the i th atom; M is a matrix element that depends on the cavity mode profiles; A^{μ} encodes the anisotropy of the spin–spin interaction; and S_i^{μ}

denotes (in general) the μ th component of the spin vector at site i . We assume that all atoms are tightly confined near *fixed random positions* by external trapping lasers; *disorder* in these positions can be achieved via the use of a diffuser, as in Ref. [14].

In the argument above, we have neglected the leakage of photons out of the cavity; this neglect can be justified as long as the average photon leakage rate κ is much less than the detuning δ , which sets the rate at which cavity photons are reabsorbed into the laser. However, the presence of dissipation, and the consequent flux of energy through the system, imply that the atom–cavity system is in general not in equilibrium. This raises the question of whether equilibrium statistical mechanics is applicable to such systems at all. We have addressed this question in previous work [15,16], and found that (provided $\kappa \ll \delta$) the primary effect of dissipative processes is to set a lifetime $\tau \propto 1/\kappa$ for the experiment. In particular, when the temperature T is zero, one can show explicitly [16] that adiabatic switching [17] holds to a good approximation on time-scales shorter than τ , and thus that the ground state of a system of uncoupled spins evolves into the ground state of the interacting system; hence, equilibrium statistical mechanics is expected to describe the system reliably in this regime.

Following the arguments given in the first paragraph of this section, the general spin Hamiltonian H_{mm} for a collection of atoms in a multimode cavity is of the following form:

$$H_{\text{mm}} = -\zeta \sum_{\alpha, i \neq j, \mu} \Xi_{\alpha}(\mathbf{x}_i) \Xi_{\alpha}(\mathbf{x}_j) A^{\mu} S_i^{\mu} S_j^{\mu} + \dots, \quad (1)$$

where $\zeta \equiv (\Omega^2 g^2)/(\Delta^2 \delta)$ is an effective coupling parameter in which Ω^2 is the laser intensity; g is the atom–cavity coupling strength, which is assumed to be the same for all modes in some quasi-degenerate family indexed by α ; and Ξ_{α} is the normalized mode function of mode α . (For the specific setup treated in Ref. [8], the spins are planar and their interactions are isotropic.) A particularly appealing feature of the cavity QED realization is that the spin–spin interaction strength can be tuned, even very rapidly, during the course of an experiment, by altering the laser intensity.

The ellipses in Equation (1) represent terms that do not involve the pump laser; these terms can typically be either compensated for via redefinitions or neglected to leading order [16]. Of these, the leading term is of the form $(g^2/\Delta) \sum_{\alpha, i} \Xi_{\alpha}(\mathbf{x}_i)^2 S_i^z$, which acts as an effective magnetic field (and stems from the shift in the cavity resonance frequency because of the presence of atoms in the cavity); one can cancel out this field via an appropriate choice of the atomic level spacing and microwave driving frequencies. The next-to-leading term, on the other hand, can generate spin–spin interactions, and takes the following form:

$$H_2 \sim \frac{g^4}{\Delta^2 \delta} \sum_{\alpha \neq \beta, i \neq j} \Xi_{\alpha}(\mathbf{x}_i) \Xi_{\beta}(\mathbf{x}_j) \Xi_{\alpha}(\mathbf{x}_j) \Xi_{\beta}(\mathbf{x}_i) S_i^z S_j^z + (\alpha \leftrightarrow \beta). \quad (2)$$

Thus, this term generates an Ising-type spin–spin interaction, which could in principle compete with the term in Equation (1). For typical cavities, one expects this term to be smaller by a few orders of magnitude than the laser-mediated coupling;

however, in the limit of very strong atom–cavity coupling, this competition is expected to modify the physics discussed in Ref. [8] and in the present work.

As cavity modes are generically oscillatory in all directions, the probability distribution of the values of $\Xi_\alpha(\mathbf{x}_i)$ for randomly located positions \mathbf{x}_i is generically peaked at ± 1 (see, e.g., Ref. [18]). We shall thus approximate the mode functions as ± 1 , as in the neural-network models; in this approximation, H_{mm} has the structure of a Hopfield neural-network model [10,11].

The Hopfield model [10] and its generalizations [9,19] are stylized descriptions of neural networks that encode associative memories. Such networks consist of N neurons that collectively store p patterns; each stored pattern is a configuration of neurons (with each neuron being “on” or “off” in the Hopfield model). The model is said to *store* a memory if, starting from any configuration sufficiently like one of the stored patterns, the zero-temperature dynamics invariably drives the system to the relevant stored pattern. In terms of a spin system, the number of patterns stored in the associative memory is the multiplicity of its local free-energy minima, or (at $T=0$) of its (non-symmetry-related) ground states. The system’s success at retrieving patterns depends on whether, and how rapidly, it is able to approach these minima. For $p=1$, it can be seen that the interactions are unfrustrated; thus the ground state is unique up to symmetry: it has the spins of all the atoms at even antinodes of the solitary cavity mode pointing in some direction, and all the spins of atoms at the odd antinodes pointing in the opposite direction (see Figure 1b). On the other hand, for $p \gg N$, the spin–spin interactions become pairwise uncorrelated, so that Equation (1) describes the Sherrington–Kirkpatrick model [20], the ground state of which is a spin glass. It is intuitively clear that a spin glass cannot encode an associative memory because of its slow dynamics and large number of metastable states [20,21]. In general, there is a transition between these phases at some finite value of p/N [9,11,19]. In the atom–cavity setting, p represents the number of cavity modes that couple strongly to the atoms; thus, by tuning the cavity geometry, one can increase p until the associative memory no longer functions.

2.1. Ring cavity and the van Hemmen model

We now consider the simplest nontrivial example of an associative memory, viz., that involving Ising spins coupled to two cavity modes. A specific realization of such a geometry is the ring cavity, which supports two degenerate modes $\Xi_\pm(x) \sim e^{\pm ikx}$. In this case the interaction term takes the translation-invariant form

$$H_{\text{ring}} = -\zeta \sum_{i < j} \cos[k(x_i - x_j)] S_i S_j. \quad (3)$$

Note that Equation (3) is an infinite-ranged approximation to the RKKY interaction; cf. Equation (1) of Ref. [18]. For a uniform distribution of positions, Equation (3) is, in effect, a realization of the van Hemmen model [12], which a particularly simple case of a Hopfield associative memory. The origins of frustration in the van Hemmen model can be understood via the illustration in Figure 2: each spin interacts ferromagnetically with those at distances less than $\lambda/2$, antiferromagnetically with those at distances between $\lambda/2$ and $3\lambda/2$, and so on. Thus, frustrated

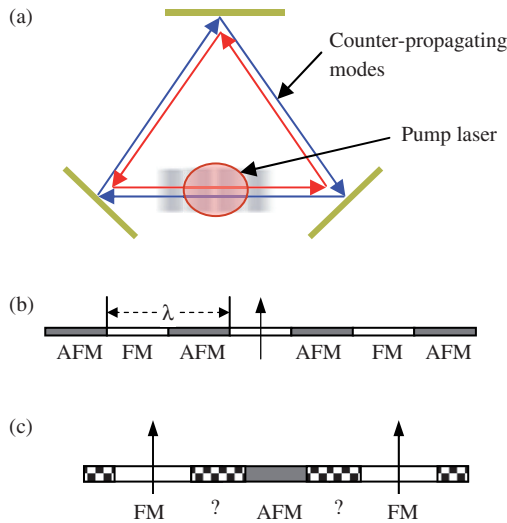


Figure 2. (Color online). (a) The ring cavity geometry, showing two degenerate, counter-propagating modes. The pump laser is taken to be oriented perpendicular to the plane of the figure, as shown. (b) Variation of the sign of the spin–spin potential due to a single Ising spin (the vertical arrow) in a ring cavity: spins in the white regions experience a ferromagnetic interaction with the pictured spin, whereas those in the grey regions experience an antiferromagnetic interaction. (c) Sign of the interaction experienced by a third spin due to two spins (the vertical arrows) positioned as shown in the figure. The two spins shown interact ferromagnetically and are therefore aligned; however, a third spin located in the patterned regions would be frustrated, as it would interact ferromagnetically with one of the depicted spins and antiferromagnetically with the other.

three-spin configurations are generic, as shown in Figure 2, for a uniform distribution of atom locations.

3. Exploring properties of associative memories

We now briefly describe how the main features of associative memories – viz., the character of the ground state, the elementary excitations, and the magnetic (or equivalent) susceptibility – can be probed experimentally in the cavity-based setting. The first of these is the most straightforward to measure, as the ground state overlaps macroscopically with the stored patterns [11], which correspond to cavity mode functions. This macroscopic overlap leads, as in the related problem of cavity-induced self-organization [15,16,22,23], to the superradiant emission of photons from the cavity in the ordered phase. In other words, the onset of the associative-memory phase should be accompanied by a sharp rise in the number of photons leaking out of the cavity. Different ground states can be distinguished by measuring (a) the spatial distribution of the emitted light [15,16], as well as (b) the relative phase between the laser light and the light emitted from the cavity [23]. Moreover, one can check that the symmetry-breaking is indeed spontaneous by subjecting the atoms to a pulse of thermal light that is resonant with one of the

atomic transitions [23], thereby randomizing the spin distribution; in the spin glass regime, the state that the system selects once the thermal light is removed should vary from shot to shot. (This is analogous to melting and refreezing the spin degrees of freedom while maintaining the specific instance of positional disorder.)

Unlike conventional magnetically ordered phases, associative memories have a high density of low-energy excitations, which contribute to the low-temperature heat capacity – e.g., in the van Hemmen case [13], the heat capacity is linear at low temperatures. In the atom–cavity system, it is more straightforward to probe the density of excitations directly, via the following spectroscopic technique [24], than to measure the heat capacity. One applies a probe laser beam that is much weaker, but at a slightly higher frequency $\omega_L + \Delta\omega$, than the pump laser beam. The rate at which photons from the probe laser beam are absorbed (i.e., transferred into the pump beam) by the atomic cloud depends on the density of spin excitations at a frequency $\Delta\omega$; by measuring the absorption rate as a function of $\Delta\omega$, one can deduce the spectral function and thus the heat capacity.

Next, we discuss how the spin susceptibility can be accessed. A preliminary step towards measuring the spin susceptibility is, of course, the application of (the analogue of) a magnetic field to the spin system; this can be accomplished by directly driving the transitions amongst the atomic levels that constitute the spin states, using microwaves. The magnetization can then be measured via spin-selective imaging techniques such as phase-contrast imaging [25]. An important technical subtlety should be noted here: in most schemes, such as the Λ atom scheme proposed in Ref. [8], the various spin states into which the system can order are different superpositions of the microscopic atomic levels; however, the spin-selective imaging techniques image the populations in individual *microscopic* levels. Thus, it is typically necessary to apply a $\pi/2$ microwave pulse to the system before imaging it.

Finally, we briefly mention how one can introduce “errors” into the ordered phase and thus investigate the robustness of the associative memory to these errors. One possible protocol is as follows: starting in the low-temperature, memory-encoding phase, one uses a local spin-addressing scheme (see, e.g., Ref. [5]) to flip all the spins in a certain region of the system. After this, one monitors the flux of photons out of the cavity as a function of time, and measures the time-scale on which this flux achieves its steady-state value: this would correspond to the system having fully *retrieved* the stored pattern. By using a combination of local spin-addressing and phase-contrast imaging, one can also more generally measure spin relaxation rates.

4. Concluding remarks

In this work we have schematically introduced an atom–cavity setting in which the physics of associative memories and related phases, such as spin glasses, can be realized and explored. This setting differs from most condensed-matter settings in that the microscopic Hamiltonian describing the system is precisely known, and the strength and structure of interactions can be tuned via the laser strength and cavity geometry, respectively; moreover, it also differs from conventional ultracold atomic settings in that the interactions are long-ranged and sign-changing in character.

In addition to outlining how such phases can be realized, we have described various schemes for measuring properties such as their ground-state degeneracies, excitation spectra, susceptibilities, and efficacy at retrieving stored patterns. We note that a prospect of particular interest raised by the current realizations is that they pave the way for exploring the physics of associative memories, as well as spin glasses, in the *quantum* regime [26].

Acknowledgments

It is a pleasure and an honor for the authors to respectfully dedicate this paper to David Sherrington, with admiration for his profound, wide-ranging and inspiring scientific contributions. One of the authors (PMG) wishes to express (or, better still, re-express – see Ref. [27]) his deep and abiding personal gratitude to David for his generous encouragement and warm friendship, beginning nearly three decades ago. The authors gratefully acknowledge support from awards DOE DE-FG02-07ER46453 (SG) and NSF DMR 09-06780 (PMG), as well as from the David and Lucille Packard Foundation (BLL).

References

- [1] I. Bloch, J. Dalibard and W. Zwerger, *Rev. Mod. Phys.* 80 (2008) p.885.
- [2] D. Rugar, R. Budakian, H.J. Mamin and B.W. Chi, *Nature* 430 (2004) p.329.
- [3] W.S. Bakr, A. Peng, M.E. Tai, R. Ma, J. Simon, S. Fölling, L. Pollet and M. Greiner, *Science* 329 (2010) p.547.
- [4] J.F. Sherson, C. Weitenberg, M. Endres, M. Cheneau, I. Bloch and S. Kuhr, *Nature* 467 (2010) p.68.
- [5] C. Weitenberg, M. Endres, J.F. Sherson, M. Cheneau, P. Schauss, T. Fukuhara, I. Bloch and S. Kuhr, *Nature* 471 (2011) p.319.
- [6] J. Struck, C. Ölschläger, R. Le Targat, P. Soltan-Panahi, A. Eckardt, M. Lewenstein, P. Windpassinger and K. Sengstock, *Science* 333 (2011) p.996.
- [7] D.M. Weld, P. Medley, H. Miyake, D. Hucul, D.E. Pritchard and W. Ketterle, *Phys. Rev. Lett.* 103 (2009), Article No. 245301.
- [8] S. Gopalakrishnan, B.L. Lev and P.M. Goldbart, arxiv:1108.1400 (2011).
- [9] J. Cook, *J. Phys. A: Math. Gen.* 22 (1989) p.2057.
- [10] J.J. Hopfield, *Proc. Nat. Acad. Sci.* 79 (1982) p.2554.
- [11] D.J. Amit, H. Gutfreund and H. Sompolinsky, *Phys. Rev. Lett.* 55 (1985) p.1530.
- [12] J.L. van Hemmen, *Phys. Rev. Lett.* 49 (1982) p.409.
- [13] J.L. van Hemmen, A.C.D. van Enter and J. Canisius, *Z. Phys. B* 50 (1983) p.331.
- [14] M. Pasienski, D. McKay, M. White and B. DeMarco, *Nature Phys.* 6 (2010) p.677.
- [15] S. Gopalakrishnan, B.L. Lev and P.M. Goldbart, *Nature Phys.* 5 (2009) p.845.
- [16] S. Gopalakrishnan, B.L. Lev and P.M. Goldbart, *Phys. Rev. A* 82 (2010), Article No. 043612.
- [17] A.A. Abrikosov, L.P. Gorkov and I.M. Dzyaloshinski, *Methods of Quantum Field Theory in Statistical Physics*, Prentice-Hall, Englewood Cliffs, NJ, 1963.
- [18] M.B. Weissman and P.G. Wolynes, *Phys. Rev. B* 46 (1992) p.14209.
- [19] Y. Nakamura, K. Torii and T. Munakata, *Phys. Rev. E* 51 (1995) p.1538.
- [20] D. Sherrington and S. Kirkpatrick, *Phys. Rev. Lett.* 35 (1975) p.1792.
- [21] K. Binder and A.P. Young, *Rev. Mod. Phys.* 58 (1986) p.801.
- [22] P. Domokos and H. Ritsch, *Phys. Rev. Lett.* 89 (2002), Article No. 253003.
- [23] A.T. Black, H.W. Chan and V. Vuletić, *Phys. Rev. Lett.* 91 (2003), Article No. 203001.

- [24] J.M. Pino, R.J. Wild, P. Makotyn, D.S. Jin and E.A. Cornell, *Phys. Rev. A* 83 (2011), Article No. 033615.
- [25] M. Vengalattore, S.R. Leslie, J. Guzman and D.M. Stamper-Kurn, *Phys. Rev. Lett.* 100 (2008), Article No. 170403.
- [26] P. Strack and S. Sachdev, arxiv:1109.2119 (2011).
- [27] P.M. Goldbart, *J. Phys. A: Math. Theor.* 41 (2008) p.1.